# Measuring the in-plane thermal diffusivity of moving samples using laser spot lock-in thermography

M. Colom[1], A. Bedoya[1,2], A. Mendioroz[1] and A. Salazar[1,*]

[1]Departamento de Física Aplicada I, Escuela de Ingeniería de Bilbao, Universidad del País Vasco UPV/EHU, Plaza Ingeniero Torres Quevedo 1, 48013 Bilbao, Spain.

[2]Instituto Politécnico Nacional (IPN), Centro de Investigación en Ciencia Aplicada y Tecnología Avanzada (CICATA), Unidad Legaria, Legaria 694, Col. Irrigación, C.P. 11500, Ciudad de México, Mexico.

*Corresponding author, E-mail address: agustin.salazar@ehu.es

**Abstract**

In this work we deal with samples that move at constant speed and are illuminated by a modulated and focused laser beam. We have obtained a general expression for the surface temperature of these moving samples: it is valid not only for opaque and thermally thick materials, but also for thermally thin and semitransparent samples. Moreover, heat losses by convection and radiation are taken into account in the model. Numerical calculations indicate that the temperature (amplitude and phase) profiles in the directions parallel and perpendicular to the sample motion are straight lines with respect to the distance to the laser spot. The slopes of these straight lines depend on sample speed, modulation frequency and in-plane thermal diffusivity of the sample. Provided the two first experimental parameters are known, the in-plane thermal diffusivity can be retrieved in a simple manner. Measurements performed on materials covering a wide range of thermal diffusivity values, from insulators to good thermal conductors, confirm the validity of these linear methods.

**Keywords:** infrared thermography, lock-in thermography, thermal diffusivity, photothermal techniques.

# 1. Introduction

Thermal diffusivity measures the speed of heat conduction inside a material during changes of temperature with time and therefore is the quantity that governs heat conduction in non steady-state conditions [1]. Accordingly, it is crucial to characterize the thermal diffusivity of new materials to understand dynamic processes in applied science and engineering. During the last decades, several research groups have developed reliable methods to measure the thermal diffusivity of materials both in the through-thickness and in the in-plane directions [2]. In particular, optically excited infrared (IR) thermography is a fully non-contact technique which provides direct methods to obtain the thermal diffusivity of a wide variety of materials [3]. These methods can be divided into two main groups (each of them can be used in time domain or in frequency domain). In the first one, the front surface of the sample is illuminated by a uniform light beam and from the analysis of either the rear or the front surface temperature the through-thickness thermal diffusivity is obtained [4-6]. In the second one, the front surface is heated by a focused laser beam and from the study of the temperature decay from the centre of the laser spot the in-plane thermal diffusivity is retrieved [7,8].

The aim of this work is to propose a method, based on laser spot lock-in thermography to measure the thermal diffusivity of samples moving at constant speed, as it is the case of in-line production or in-line inspection in factories, where heterogeneities, i.e. local changes in the properties, must be detected in real time, without stopping the production chain. Recently, we proposed a method based on laser spot IR thermography, which consists in illuminating the sample surface by a focused CW laser beam and recording the surface temperature by an IR video camera [9,10]. We found that the temperature profiles along two orthogonal directions, transverse and longitudinal to the sample movement, and crossing the centre of the laser spot show a linear behaviour from whose slope the thermal diffusivity can be obtained. The method works well, but it lacks precision especially with good thermal conductors, which produce weak signals, because the uncertainty in the experiments is determined by the intrinsic noise of the camera (around 20 mK).

In this work, we propose to use a modulated laser spot to heat the sample surface and to take advantage of the lock-in process to obtain the thermal diffusivity of moving samples with high accuracy. This is due to the noise reduction (below 1 mK) provided by the lock-in analysis of a large number of frames. First, we have obtained an analytical expression for the front surface temperature of a solid which is illuminated by a modulated and focused laser beam. The solution is general in the sense that it is valid for both opaque and transparent materials and also

for thermally thick and thin samples. The equation also incorporates heat losses by convection and radiation. From systematic numerical calculations, we have found that the two central temperature profiles, in the direction of the sample motion and in the direction perpendicular to it, behave linearly as a function of the distance to the laser spot. We have found closed expressions for their slopes, which depend on the modulation frequency and on the speed and thermal diffusivity of the sample. Provided the two first experimental parameters are known, the thermal diffusivity can be retrieved. Laser spot lock-in thermography measurements on calibrated samples covering a wide range of thermal diffusivities confirm the validity of these linear methods.

## 2. Theory

In this section we calculate the surface temperature of a homogeneous and isotropic sample moving along the *x*-axis at constant speed *v* when its surface is illuminated by a CW laser of Gaussian profile modulated at a frequency $f$ ($\omega = 2\pi f$). The geometry of the problem is shown in Fig. 1. The starting point is the expression of the surface temperature of a sample at rest, which is illuminated by a brief laser pulse [11]. Then, a convolution product of this expression provides the surface temperature of a moving sample illuminated by a modulated laser beam.
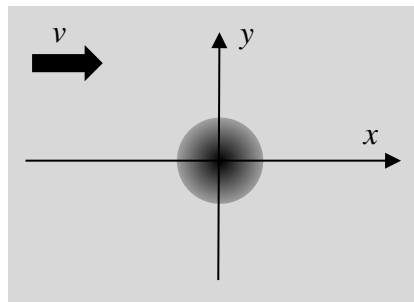


Fig. 1. Front surface of a homogeneous and isotropic sample, which is illuminated by a Gaussian laser spot. The laser remains at rest at the origin of coordinates, while the sample is moving to the right at constant speed *v*.

Equation (1) gives the expression of the time dependence of the surface temperature of a slab of thickness *L* and optical absorption coefficient $\alpha$, which is illuminated by an extremely brief laser pulse of energy $Q_o$ [11]. The laser spot has Gaussian profile of radius *a* (at $1/e^2$).

$$T(r,t) = \frac{2Q_o}{\pi} B(t) \frac{e^{-\frac{2r^2}{a^2+8Dt}}}{a^2+8Dt}, \tag{1}$$

$B(t)$ reduces to simple expressions in the following cases of interest:

(a) For an opaque and thermally thick material $B(t) = \frac{1}{\varepsilon}\left[\frac{1}{\sqrt{\pi t}} - \frac{h}{\varepsilon} e^{(h/\varepsilon)^2 t} Erfc\left(\frac{h}{\varepsilon}\sqrt{t}\right)\right].$ (2a)

(b) For an opaque and thermally thin material $B(t) = \frac{1}{\rho c L} e^{-\frac{2ht}{\rho c L}}.$ (2b)

(c) For a semitransparent material $B(t) = \frac{\alpha}{\rho c}.$ (2c)

Here $D$ and $\varepsilon$ are the thermal diffusivity and effusivity respectively, $\rho$ is the density, $c$ is the specific heat and $h$ is coefficient of heat losses by convection and radiation.

By performing a convolution product of Eq. (1) we obtain the surface temperature of a sample that is moving at constant speed to the right while a CW laser beam remains at rest

$$T(x,y,t) = \frac{2P_o}{\pi} \int_0^t B(t-\tau) \frac{e^{-\frac{2\{[x-v(t-\tau)]^2+y^2\}}{a^2+8D(t-\tau)}}}{a^2+8D(t-\tau)} d\tau, \tag{3}$$

where $P_o$ is the laser power. In this expression, the temperature is calculated at a time $t$ after the laser was switched on ($t = 0$).

Finally, if the laser is modulated at a frequency $f$, the surface temperature is given by

$$T(x,y,t,\omega) = \frac{P_o}{\pi} \int_0^t B(t-\tau) \frac{e^{-\frac{2\{[x-v(t-\tau)]^2+y^2\}}{a^2+8D(t-\tau)}}}{a^2+8D(t-\tau)} e^{i\omega\tau} d\tau. \tag{4}$$

Note that in this expression the power is divided by a factor 2 since, as the laser is modulated, only half of its power reaches the sample. As the surface temperature oscillates at the same frequency as the laser spot, Eq. (4) can be written as

$$T(x,y,t,\omega) = \theta(x,y)e^{i\omega t} = |\theta| e^{i\varphi} e^{i\omega t}, \tag{5}$$

where $\theta$ is the spatial component of the surface temperature and $|\theta|$ and $\varphi$ are its amplitude and phase respectively. Accordingly, $|\theta|$ and $\varphi$ can be obtained from Eq. (5)

$$|\theta| e^{i\varphi} = \frac{T(x,y,t,\omega)}{e^{i\omega t}}. \tag{6}$$

## 3. Numerical calculations

Figure 2a shows the profiles of the natural logarithm of the amplitude of the surface temperature and of the phase along the $y$-axis, i.e. in the direction perpendicular to the sample movement. Calculations have been performed for AISI-304 stainless steel ($D = 4$ mm$^2$/s and $\varepsilon = 7500$ Ws$^{0.5}$m$^{-2}$K$^{-1}$) illuminated by a laser beam of radius $a = 0.2$ mm and modulated at $f = 10$ Hz. Adiabatic boundary conditions are assumed ($h = 0$). The lower graphic corresponds to an opaque and thermal thick sample (Eq. 2a), while on the upper graphic the specimen is opaque and thermally thin (Eq. 2b). The same results are also obtained for a semitransparent sample. Note that to obtain straight lines the temperature amplitude is multiplied by the distance to the centre of the laser spot in the case of opaque and thermally thick samples, but by the square root of this distance in the case of opaque and thermally thin samples and also for semitransparent ones. In this figure, continuous lines stand for the sample at rest and they are parallel straight lines whose common slope $m$ is directly related to the thermal diffusivity of the sample: $m = \sqrt{\pi f / D}$. These linear relations have been used for years to measure the in-plane thermal diffusivity of solid samples [8,12]. In turn, dotted lines correspond to the calculations when the sample is moving at $v = 3$ cm/s. As can be seen, the sample movement produces a reduction of the phase slope together with an increase of the amplitude slope with respect to the static case, which are more pronounced as the sample speed increases. Systematic calculations indicate that the product of both slopes is independent of the sample speed and satisfies

$$m_{Ln(|\theta|y^n)} \times m_\varphi = \frac{\pi f}{D}, \tag{7}$$

where $n = 1$ for opaque and thermally thick samples and $n = 0.5$ for opaque and thermally thin samples and also for semitransparent materials. This equation provides a simple method to measure the thermal diffusivity of the moving sample in the transverse direction.

Figure 2b is similar to Fig. 2a, but for the profile along the $x$-axis, i.e. in the direction of the sample movement. As before, continuous lines correspond to the sample at rest and therefore they show the same behaviour as the $y$-axis profiles. Dotted lines correspond to a sample moving at $v = 3$ cm/s. The sample movement produces the same reduction of the phase slope as in the $y$-axis profile. However, the motion produces a reduction of the slope of the amplitude for $x > 0$, but an increase of the slope for $x < 0$, with respect to the sample at rest. Numerical calculations indicate that the phase slope satisfies the following expression, with an error smaller than 1%

$$m_{\varphi} = \sqrt{\frac{\pi f}{D}} \sqrt{\frac{31.90}{31.90 + \left(\dfrac{v^2}{Df}\right)^{1.1813}}} .$$

(8)

Moreover, the slope of the right branch of the amplitude verifies, within the same uncertainty of 1%

$$m_{Ln(|\theta|x^n)} = \sqrt{\frac{\pi f}{D}} \exp\left[-\frac{\pi}{10}\left(\frac{v^2}{Df}\right)^{0.55}\right].$$

(9)

As before, $n = 1$ for opaque and thermally thick samples and $n = 0.5$ for opaque and thermally thin samples and also for semitransparent ones. From Eqs. (8) and (9) the thermal diffusivity of the sample along the $x$-axis can be obtained.
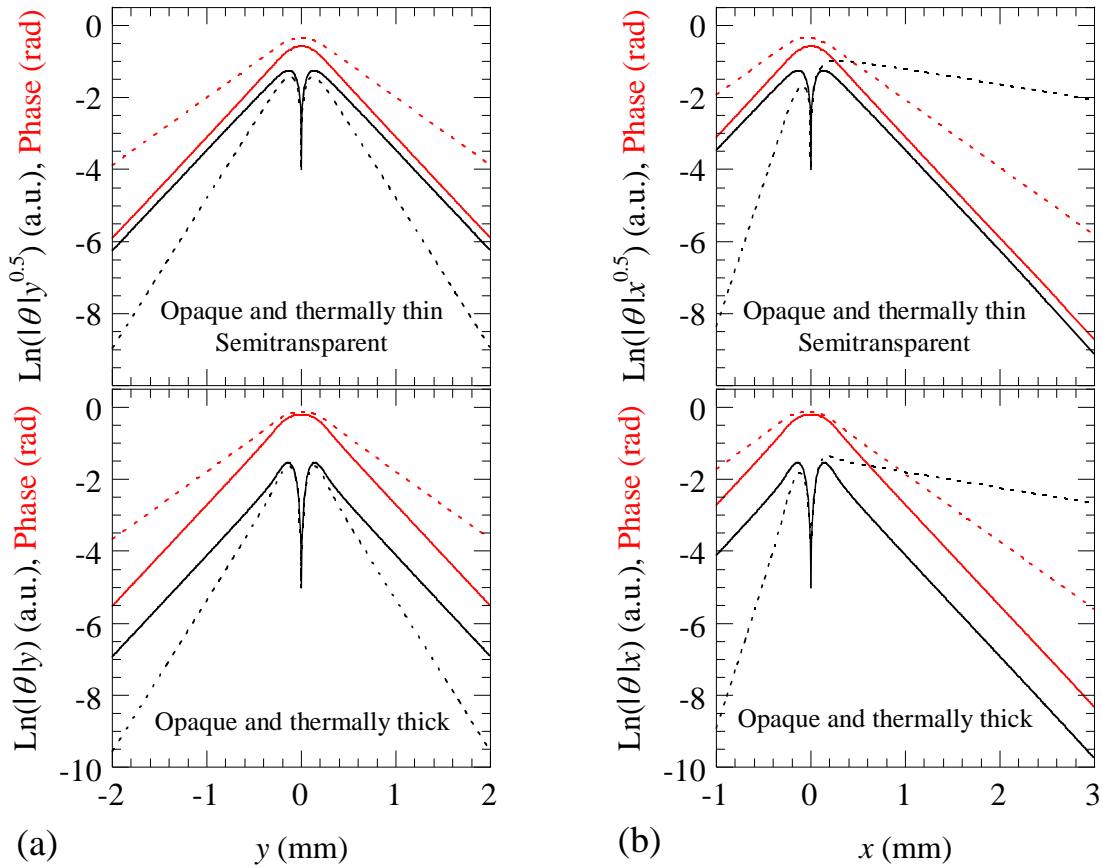


Fig. 2. Calculations of the amplitude and phase profiles of the surface temperature along the $y$-axis (a) and $x$-axis (b). The bottom row corresponds to an opaque and thermally thick sample. The upper row corresponds to an opaque and thermally thin sample or to a semitransparent sample. Continuous lines: the sample is at rest; dotted lines: the sample is moving at $v = 3$ cm/s. Calculations have been performed for AISI-304 stainless steel ($D = 4$ mm$^2$/s and $\varepsilon = 7500$ Ws$^{0.5}$m$^{-2}$K$^{-1}$) heated by a laser beam of radius $a = 0.2$ mm modulated at $f = 10$ Hz, in adiabatic boundary conditions ($h = 0$).

The linear relations given in Eqs. (7) to (9) are obtained assuming that the sample has reached the steady state, i.e. $t = \infty$ in the convolution integral in Eq. (4). In order to apply those linear relations to obtain the thermal diffusivity of moving samples, we have to analyse which is the minimum time after switching on the laser ($t_{min}$) required for the sample to reach the steady state. As $t_{min}$ depends on the distance to the laser spot (the larger this distance, the longer $t_{min}$) we take as reference a distance ten times larger than the thermal diffusion length, $10\sqrt{\dfrac{D}{\pi f}}$. We consider that the sample has reached the steady state when the temperature differs by less than 0.1% with respect to the temperature at $t = \infty$. In Fig. 3 we show the numerical calculations of $t_{min}$ as a function of the sample speed. Thermal diffusivity values covering a wide range from thermal insulators to good thermal conductors have been considered. It is worth noting that for a given couple ($D,v$) $t_{min}$ is independent of the modulation frequency. As can be observed, the higher the velocity the shorter $t_{min}$. Actually, it is well known that for samples at rest, the laser must be switched on for several minutes before conducting modulated experiments. On the other hand, the steady state is reached faster for thermal insulators than for good thermal conductors. Anyway, for speeds of several cm/s, which are those expected in real applications in in-line production in factories, the steady state is reached in few seconds.
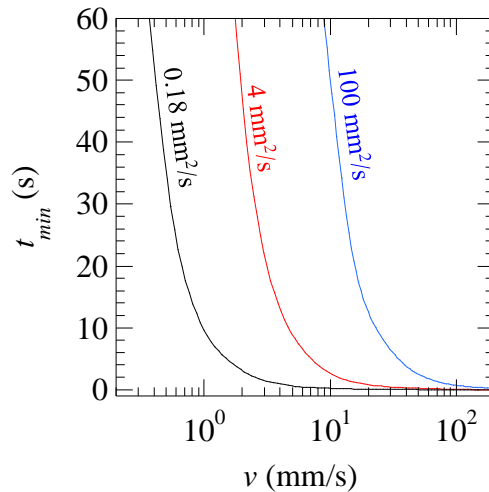


Fig. 3. Numerical calculation of the minimum time needed for the sample to reach the steady state once the laser is switched on, as a function of the sample speed. Calculations are performed for three thermal diffusivity values.

In order to study the accuracy of the thermal diffusivity values obtained from the linear relations corresponding to Eqs. (8) and (9), we analyse the sensitivity of these equations to

thermal diffusivity. In particular, we evaluate how the error in the slope, $\Delta m$, is transmitted to an error in the estimated diffusivity, $\Delta D$. The results for Eq. (8), corresponding to the phase slope, are shown in Fig. 4a. Calculation are performed for several values of the dimensionless factor $\dfrac{v^2}{Df}$. As can be observed, the best situation occurs when this dimensionless factor is very small i.e. when the sample is at rest or moving at very low speed or the modulation frequency is very high. In this case $\Delta D = 2\,\Delta m$. As the factor increases, the error in diffusivity dramatically increases. For instance, for $\dfrac{v^2}{Df} = 25$, $\Delta D \approx 6.5\,\Delta m$, but for $\dfrac{v^2}{Df} = 64$ then $\Delta D \approx 50\,\Delta m$. These results indicate that the reliability of the slope method to obtain $D$ decreases as the dimensionless factor increases. Consequently, we have stablished an upper limit for this factor: the method is valid provided $\dfrac{v^2}{Df} < 25$. According to this limit, reaching high speeds requires using high enough frequencies. This is easy to fulfil in the case of good thermal conductors, but in the case of thermal insulators the modulation frequency is limited by the spatial resolution, so for insulators it is difficult to work at $v > 1$ cm/s.
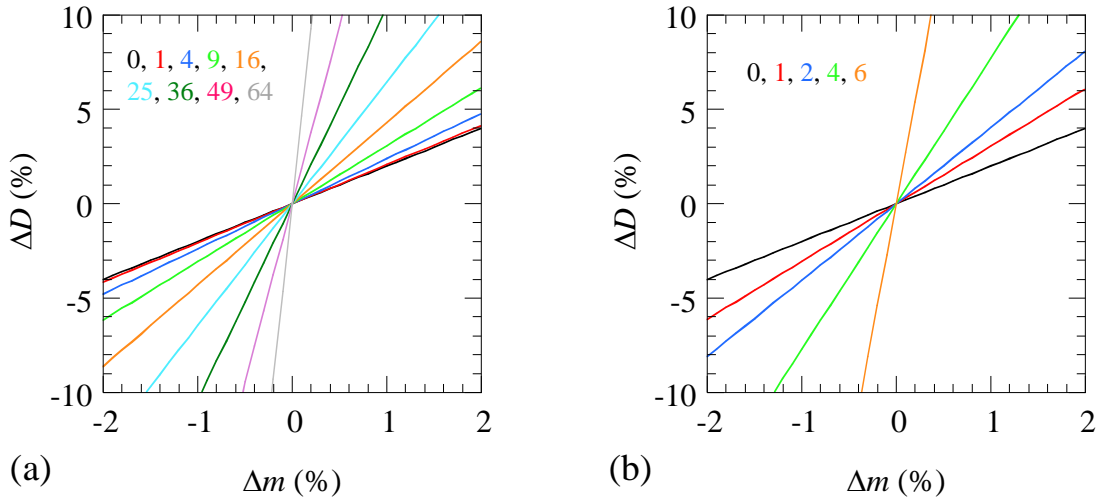


(a)

(b)

Fig. 4. (a) Numerical calculation of the error transmission from phase slope to thermal diffusivity value according to Eq. (8). Calculations are performed for several values of the factor $\dfrac{v^2}{Df}$. (b) The same for Eq. (9) corresponding to the amplitude slope.

We have performed the same analysis for Eq. (9), which corresponds to the amplitude slope. The results are shown in Fig. 4b. As can be seen, even for very small values of the dimensionless factor the error in diffusivity is huge. Accordingly, we dismiss the amplitude slope to measure the thermal diffusivity of moving samples.

Finally, we study the effect of heat losses due to convection and radiation on the linear relations we propose to measure the thermal diffusivity of moving samples. According to Eq. (2a), corresponding to opaque and thermally thick samples, the coefficient of heat losses is correlated to the sample effusivity. This means that the effect of heat losses is more pronounced for thermal insulators than for thermal conductors, as is also the case in a static situation. On the other hand, the effect of heat losses increases at low frequencies and/or low sample speeds. Numerical calculations indicate that in the presence of heat losses the linearity of the amplitude and phase profiles is preserved, but the slopes given by Eqs. (7) to (9) are slightly modified. Anyway, for realistic values of the coefficient of heat losses at room temperature ($h = 10 - 15$ $Wm^{-2}K^{-1}$) [13] and sample speed higher than 4 mm/s, the influence of heat losses on the retrieved thermal diffusivity is negligible.

In the case of opaque and thermally thin samples, see Eq. (2b), the coefficient of heat losses is correlated to the product $\rho c L$. As the heat capacity in solids ($\rho c$) is bounded between $10^6$ and $4 \times 10^6$ $Jm^{-3}K^{-1}$ [1], the effect of heat losses mainly depends on the sample thickness and therefore it could be significant for very thin samples. However, numerical calculations show that heat losses reduce the phase slope and increase the amplitude slope, in such a way that the product of slopes still satisfies Eq. (6), as is the case of thin samples at rest [14,15].

In the case of semitransparent samples the surface temperature is not affected by heat losses as can be seen in Eq. (2c).

## 4. Experimental results and discussion

To verify the ability of the linear methods (Eqs. (7) and (8)) to measure the thermal diffusivity on moving samples we have used the IR thermography setup drawn in Fig. 5. A CW laser (532 nm, up to 6 W) is modulated by a mechanical chopper and focused on the sample surface with a 10 cm focal length lens to a radius of about 200 $\mu$m. A Ge window, which reflects visible light and transmits IR wavelengths, is used to direct the laser beam perpendicularly to the sample and, at the same time, to prevent the scattered laser radiation from reaching the IR camera. An IR video camera (FLIR, model SC7500, 320 × 256 pixels, pitch 30 $\mu$m and spectral band from 3 to 5 $\mu$m) records the temperature field at the sample surface. The Ge window is

transparent to wavelengths longer than 2 µm. Moreover, an anti-reflection coating enhances its transmission to mid infrared wavelengths above 95%. A lock-in module transforms the recorded film into an amplitude thermogram and a phase thermogram. An IR microscope lens is used to improve the spatial resolution of the IR camera up to 30 µm, with a field of view of 9.60 mm x 7.68 mm. The sample is mounted on a dynamic system (cart + track) that is coupled to an electric engine to move the cart at constant speed.
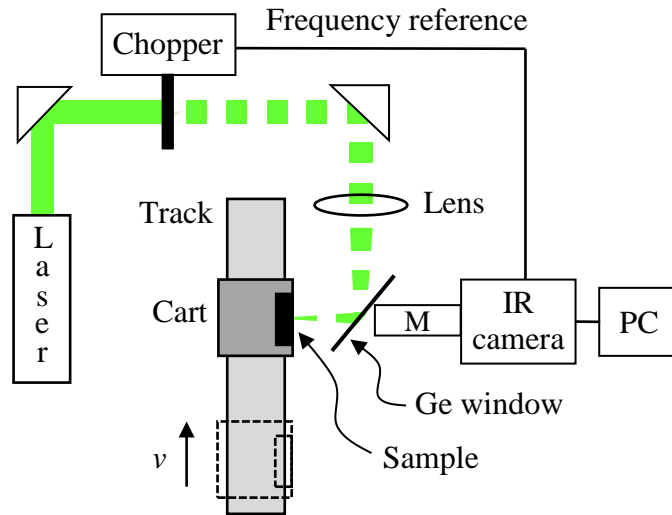


Fig. 5. Scheme of the infrared thermography setup with the sample moving at constant speed while the modulated laser beam remains at rest.

We work with 20-30 cm long samples and the modulated laser illuminates the moving sample at all times. In order to guarantee that the steady state has been reached, only the frames recorded during the passage of the second half of the sample in front of the camera are analysed in the lock-in process.

We have tested several samples covering a wide range of thermal diffusivities, from thermal insulators to good thermal conductors. Moreover, opaque, semitransparent, thick and thin samples have been analysed. In the case of opaque samples, the illuminated surface is covered by a thin graphite layer to avoid heterogeneities in the surface emissivity. At the same time, this layer enhances the laser absorptivity and the infrared emissivity, thus improving the signal to noise ratio.

Figure 6 shows the amplitude and phase thermograms corresponding to a Poly-Ether-Ether-Ketone (PEEK) sample moving to the right at $v = 9$ mm/s. The sample is illuminated by a fixed laser spot modulated at $f = 6$ Hz. As can be observed, the amplitude shows an elongated

shape due to the dragging effect produced by the sample movement. The phase, instead, shows a symmetric shape, i.e. the isophases are concentric and equidistant circumferences. In order to obtain the thermal diffusivity we analyse the amplitude and phase profiles along the longitudinal and transverse directions.
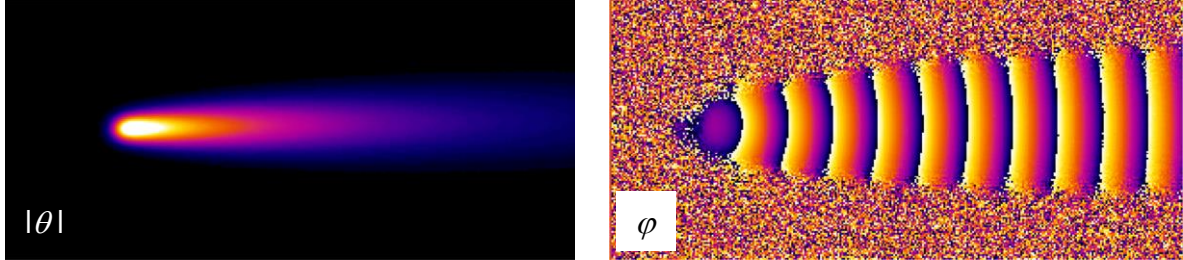


Fig. 6. Experimental thermograms of the amplitude and phase of the surface temperature for a PEEK sample moving to the right at $v = 9$ mm/s when it is illuminated by a laser spot of radius $a = 0.2$ mm modulated at $f = 6$ Hz which remains at rest.

Figure 7 shows the longitudinal phase profiles for an AISI-304 stainless steel sample 3 mm thick. To assess the robustness of the method we have performed several measurement varying the speed and the frequency, but preserving the criterion $\frac{v^2}{Df} < 25$. For all the frequencies used in the experiments the sample behaves as thermally thick. Dots are the experimental data and the continuous lines the linear fits. As can be observed, the linearity is very good and the retrieved thermal diffusivity values are the same within the experimental uncertainty ($D = 3.9 \pm 0.2$ mm$^2$/s) and in agreement with the acknowledged value for this alloy (see Table 1).

In Fig. 8, we show the longitudinal phase profiles for seven samples covering a wide range of thermal diffusivities. Three of them are opaque and thermally thick samples (PEEK, AISI-304 and graphite), two are semitransparent (orange Poly-Methyl-Methacrylate (PMMA) and amber PEEK) and two are opaque and thermally thin (0.2 mm thick AISI-304 and 0.2 mm thick graphite). As before, the couple speed and frequency is selected fulfilling the criterion $\frac{v^2}{Df} < 25$: opaque and thick PEEK (5 mm/s, 7 Hz), thick AISI-304 (8 cm/s, 80 Hz), thick graphite (10 cm/s, 18 Hz), orange PMMA (2.5 mm/s, 3 Hz), amber PEEK (5 mm/s, 4 Hz), thin AISI-304 (1.5 cm/s, 6 Hz) and thin graphite (10 cm/s, 13 Hz). Note that the phase linearity

extends for many radians (over more than 20 radians in the case of thermal insulators) due to the slow reduction of the temperature amplitude in the direction of the sample motion (see the amplitude thermogram in Fig. 6). The retrieved thermal diffusivity values are summarized in the third column of Table 1 and agree very well with the literature values. Note that for graphite we have different values for the thick sample ($L = 9$ mm) and for the thin one ($L = 0.2$ mm). This result is confirmed by independent measurements performed by static laser spot lock-in thermography [8] and by laser flash technique [4].
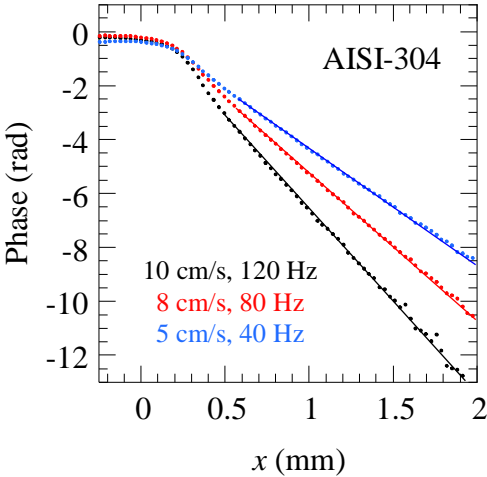


Fig. 7. Experimental longitudinal phase profiles for AISI-304. Dots are the experimental data and the continuous lines the linear fits. Three couples ($v$, $f$) have been used to evaluate the robustness of the method.
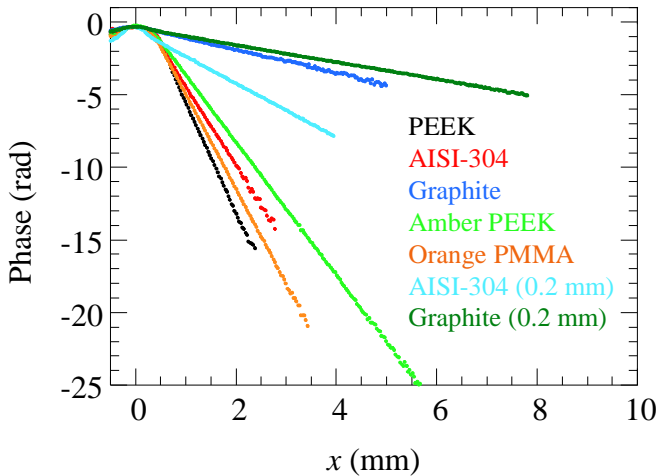


Fig. 8. Experimental longitudinal phase profiles for seven samples measured in this work.

12

Finally, the transverse amplitude and phase profiles are shown in Fig. 9. Only the results for AISI-304 stainless steel and graphite are shown, since the transverse profiles for thermal insulators, due to the lack of spatial resolution, are not usable for reliable thermal diffusivity measurements. Dots are the experimental data and the continuous lines the linear fits. The thermal diffusivity values obtained using Eq. (7) are given in the second column of Table1. They are consistent with the values obtained from the longitudinal profiles and agree with the literature values.
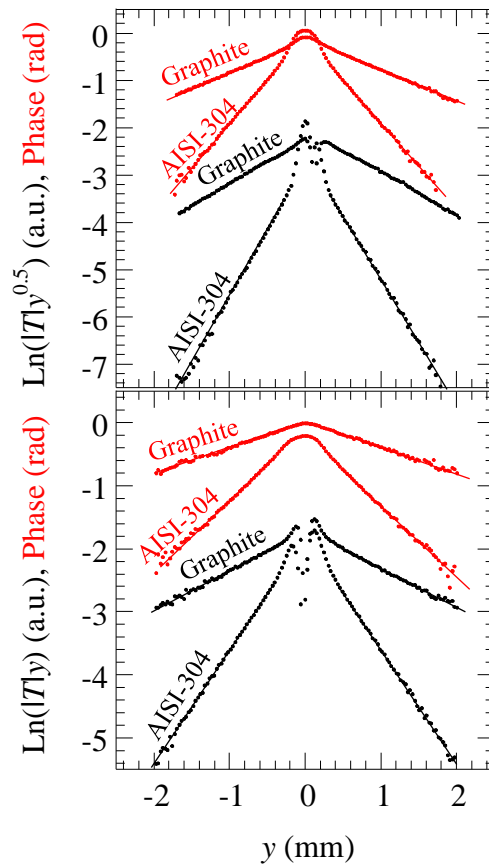


Fig. 9. Experimental transverse amplitude and phase profiles for AISI-304 stainless steel and graphite. The bottom figure corresponds to thermally thick samples while the upper figure is for thermally thin samples ($L = 0.2$ mm). Dots are the experimental data and the continuous lines the linear fits.

One of the main advantages of the methods proposed in this work is that they are based on simple linear relations. They do not require complex multiparametric fittings, since the linearity is independent of the laser radius and of heat losses. Moreover, these methods do not involve absolute measurement of the surface temperature, which is a challenging task requiring

the knowledge of the surface emissivity. In fact, the only constraint for the IR sensor is to be linear in the whole temperature range of the experiment.

We would like to stress that these linear methods are also valid for anisotropic materials if the direction of motion coincides with one of the principal axes. This is because anisotropic samples behave as isotropic along the principal directions.

**Table 1.** Retrieved thermal diffusivities ($mm^2$/s) using the linear methods proposed in this manuscript. The first set corresponds to opaque and thermally thick samples, the second set to semitransparent samples and the third one to opaque and thermally thin samples.

| Sample | $D$ (Transverse profile) | $D$ (Longitudinal profile) | $D$ (Literature) [16-19] |
|---|---|---|---|
| PEEK | - | $0.18 \pm 0.01$ | 0.18 |
| AISI-304 | $4.0 \pm 0.3$ | $3.9 \pm 0.2$ | 4.0 |
| Graphite | $55 \pm 3$ | $60 \pm 2$ | 57*·** |
| | | | |
| Orange PMMA | - | $0.105 \pm 0.005$ | 0.11 |
| Amber PEEK | - | $0.18 \pm 0.01$ | 0.18 |
| | | | |
| AISI-304 ($L = 0.2$ mm) | $3.8 \pm 0.3$ | $3.7 \pm 0.2$ | 4.0 |
| Graphite ($L = 0.2$ mm) | $76 \pm 4$ | $76 \pm 2$ | 74* |

*Measured by a static lock-in thermography setup.
**Measured by the laser flash technique.

The results obtained in this work confirm the ability of laser spot lock-in thermography to be used in in-line production or in-line inspection to measure the thermal diffusivity without stopping the process. It is worth remarking that in the case of good thermal conductors, as metals or alloys, it is quite easy to obtain good results at speeds in the range 10 - 15 cm/s, which are quite realistic values for samples moving in a conveyor belt in-line production. However, in the case of thermal insulators, velocities above 1 cm/s require frequencies higher than 20 Hz

in order to fulfilling the condition $\frac{v^2}{Df} < 25$. At those frequencies, due to the limited spatial resolution of our IR camera (30 μm), the amplitude and phase profiles are too short and therefore the retrieved diffusivity lacks reliability.

Before concluding this section let us compare the usefulness of the modulated excitation studied in this work, with the continuous illumination analyzed in previous papers [9,10]. Although the methods used in both configurations are very similar, since they are based on the linearity of the temperature profiles crossing the center of the laser spot, the main difference lies on the noise reduction provided by the lock-in analysis. This is especially significant in the case of good thermal conductors (see Fig. 10b in Ref. 9). Moreover, for continuous illumination the longitudinal profile, which exhibits the best signal to noise ratio, is horizontal regardless the thermal properties of the sample and therefore is useless for thermal diffusivity measurements. On the contrary, in the case of modulated illumination, this profile provides a linear phase behavior, which depends on the sample diffusivity and exhibits an excellent signal to noise ratio. Both reasons lead us to conclude that using a modulated laser beam is preferable to illuminating the sample with a continuous laser beam.

## 5. Conclusions

In the last decades, taking advantage of technological improvements in electronics, several accurate methods to measure the thermal diffusivity of solids have been developed. In this work, we have addressed the challenge of measuring the thermal diffusivity of samples that are moving at constant speed. Using a laser spot lock-in thermography setup, we have proposed two methods, based on simple linear relations, to measure the in-plane thermal diffusivity both in the direction of the sample movement and in the direction perpendicular to it. Measurements performed on samples covering a wide range of thermal diffusivities, from thermal insulators to good thermal conductors, confirm the validity of those linear methods.

## Acknowledgments

**References**

[1] A. Salazar, On thermal diffusivity, Eur. J. Phys. **24**, 351-358 (2003).

[2] B. Abad, D.A. Borca-Tasciuc, M.S. Martin-Gonzalez, Non-contact methods for thermal properties measurements, Renewable and Sustainable Energy Reviews **76**, 1348-1370 (2017).

[3] X.P.V. Maldague, Theory and practice of infrared technology for nondestructive testing, John Wiley & Sons, New York (2001).

[4] W.J. Parker, R.J. Jenkins, C.P. Butler and G.L. Abbott, Flash method of determining thermal diffusivity, heat capacity, and thermal conductivity, J. Appl. Phys. **32** 1679-84 (1961).

[5] R. Santos and L.C.M. Miranda, Theory of the photothermal radiometry with solids, J. Appl. Phys. **52**, 4194-4198 (1981).

[6] D.L. Balageas, Thermal diffusivity measurement by pulsed methods, High Temp.-High Press. **21**, 85-96 (1989).

[7] F. Cernuschi, A. Russo, L. Lorenzoni, A. Figari, In-plane thermal diffusivity evaluation by infrared thermography, Rev. Sci. Instrum. **72**, 3988-3995 (2001).

[8] L. Fabbri and P. Fenici, Three-dimensional photothermal radiometry for the determination of the thermal diffusivity of solids, Rev. Sci. Instrum. **66**, 3593-3600 (1995).

[9] A. Bedoya, J. González, J. Rodríguez-Aseguinolaza, A. Mendioroz, A. Sommier, J.C. Batsale, C. Pradere and A. Salazar, Measurement of in-plane thermal diffusivity of solids moving at constant velocity using laser spot infrared thermography, Measurement **134**, 519-526 (2019).

[10] L. Gaverina, M. Bensalem, A. Bedoya, J. González, A. Sommier, J.L. Battaglia, A. Salazar, A. Mendioroz, A. Oleaga, J.C. Batsale and C. Pradere, Constant Velocity Flying Spot for the estimation of in-plane thermal diffusivity on anisotropic materials, Int. J. Thermal Sci. **145**, 106000 (2019).

[11] N. W. Pech-May, A. Mendioroz and A. Salazar, Simultaneous measurement of the in-plane and in-depth thermal diffusivity of solids using pulsed infrared thermography with focused illumination, NDT&E International **77**, 28-34 (2016).

[12] B. Zhang and R. E. Imhof, Theoretical analysis of the surface thermal wave technique for measuring the thermal diffusivity of thin plates, Appl. Phys. A, **62**, 323-334 (1996).

[13] A. Salazar, A. Mendioroz and R. Fuente, The strong influence of heat losses on the accurate measurement of thermal diffusivity using lock-in thermography, Appl. Phys. Lett. **95**, 121905 (2009).

[14] A. Wolf, P. Pohl and R. Brendel, Thermophysical analysis of thin films by lock-in thermography, J. Appl. Phys. 96, 6306-6312 (2004).

[15] A. Mendioroz, R. Fuente-Dacal, E. Apiñaniz and A. Salazar, Thermal diffusivity measurements of thin plates and filaments using lock-in thermography, Rev. Sci. Instrum. **80**, 074904 (2009).

[16] Y.A. Çengel, Heat Transfer: A practical Approach, McGraw-Hill, Boston, (2003).

[17] Goodfellow catalogue at http://www.goodfellow.com.

[18] D.P. Almond and P.M. Patel, Photothermal Science and Techniques, Chapman & Hall, London (1996), p. 16,17.

[19] L.R. Touloukian, R.W. Powell, C.Y. Ho and M.C. Nicolasu, *Thermal Diffusivity* (IFI/Plenum, New York, 1973).